

*Note.* This article will be published in a forthcoming issue of the *Journal of Applied Biomechanics*. The article appears here in its accepted, peer-reviewed form, as it was provided by the submitting author. It has not been copyedited, proofread, or formatted by the publisher.

**Section:** Computational Model

**Article Title:** OpenSim Versus Human Body Model: A Comparison Study for the Lower Limbs During Gait

**Authors:** Antoine Falisse<sup>1</sup>, Sam Van Rossom<sup>1</sup>, Johannes Gijssbers<sup>2</sup>, Frans Steenbrink<sup>2</sup>, Ben J.H. van Basten<sup>2</sup>, Ilse Jonkers<sup>1</sup>, Antonie J. van den Bogert<sup>3</sup>, and Friedl De Groot<sup>1</sup>

**Affiliations:** <sup>1</sup>Department of Movement Sciences, KU Leuven, Leuven, Belgium. <sup>2</sup>Motekforce Link B.V., Amsterdam, The Netherlands. <sup>3</sup>Department of Mechanical Engineering, Cleveland State University, Cleveland, OH, USA.

**Journal:** *Journal of Applied Biomechanics*

**Acceptance Date:** May 4, 2018

©2018 Human Kinetics, Inc.

**DOI:** <https://doi.org/10.1123/jab.2017-0156>

## **OpenSim versus Human Body Model: a comparison study for the lower limbs during gait**

Antoine Falisse<sup>1</sup>, Sam Van Rossom<sup>1</sup>, Johannes Gijsbers<sup>2</sup>, Frans Steenbrink<sup>2</sup>, Ben J.H. van Basten<sup>2</sup>,  
Ilse Jonkers<sup>1</sup>, Antonie J. van den Bogert<sup>3</sup>, Friedl De Groot<sup>1</sup>

<sup>1</sup>Department of Movement Sciences, KU Leuven, Leuven, Belgium

<sup>2</sup>Motekforce Link B.V., Amsterdam, The Netherlands

<sup>3</sup>Department of Mechanical Engineering, Cleveland State University, Cleveland, OH, USA

**Conflict of Interest Disclosure:** Johannes Gijsbers, Frans Steenbrink, and Ben J.H. van Basten are affiliated to Motekforce Link B.V. (Amsterdam, The Netherlands).

### **Correspondence Address:**

Antoine Falisse  
Department of Movement Sciences  
Tervuursevest 101 box 1501  
BE-3001 Heverlee, Belgium  
Phone: +32.479.543.293 Email: [antoine.falisse@kuleuven.be](mailto:antoine.falisse@kuleuven.be)

**Running Title:** OpenSim vs Human Body model: a comparison study

## **Abstract**

Musculoskeletal modeling and simulations have become popular tools for analyzing human movements. However, end-users are often not aware of underlying modeling and computational assumptions. This study investigates how these assumptions affect biomechanical gait analysis outcomes performed with Human Body Model and the OpenSim gait2392 model. We compared joint kinematics, kinetics, and muscle forces resulting from processing data from seven healthy adults with both models. Although outcome variables had similar patterns, there were statistically significant differences in joint kinematics (maximal difference:  $9.8 \pm 1.5$  degrees in sagittal plane hip rotation), kinetics (maximal difference:  $0.36 \pm 0.10$  N·m/kg in sagittal plane hip moment), and muscle forces (maximal difference:  $8.51 \pm 1.80$  N/kg for psoas). These differences might be explained by differences in hip and knee joint center locations up to  $2.4 \pm 0.5$  and  $1.9 \pm 0.2$  cm in the postero-anterior and infero-superior directions, respectively, and by the offset in pelvic reference frames of about 10 degrees around the medio-lateral axis. Model choice may not influence the conclusions in clinical settings where the focus is on interpreting deviations from reference data but will affect the conclusions of mechanical analyses where the goal is to obtain accurate estimates of kinematics and loading.

**Keywords:** biomechanics, musculoskeletal modeling, simulation, static optimization

**Word count:** 3963

## Introduction

Musculoskeletal models for biomechanical simulations have become increasingly popular to analyze human movement. In addition to joint kinematics and kinetics, musculoskeletal models enable researchers and clinicians to assess other biomechanical variables such as muscle lengths and forces. Different software systems were developed for modeling and analyzing human movement (e.g. AnyBody<sup>1</sup>, OpenSim<sup>2</sup>, and Human Body Model<sup>3</sup>) and there is an increasingly large body of literature reporting analyses of motion based on these software systems. OpenSim offers several musculoskeletal models with varying complexity (e.g. number of muscles and kinematic degrees of freedom (DOFs)), therefore giving users multiple choices for their study. Roelker *et al.*<sup>4</sup> recently provided valuable information about which OpenSim model to use for studying gait by investigating the effects of using different models on joint kinematics, kinetics, and muscle function. They reported that differences between models were mainly due to different coordinate system definitions and muscle parameters and concluded that the gait2392 model is sufficiently complex to study gait in healthy adults. When interpreting differences in results obtained with different software systems, the added challenge is that discrepancies might result from differences between data processing workflows besides differences between models. To our knowledge, no studies have assessed differences in joint kinematics, kinetics and muscle forces induced by the use of different models in different software systems. In this study, we compared the clinically-oriented Human Body Model with the research-oriented OpenSim gait2392 model<sup>5</sup>. The goals of this comparison were (1) to evaluate how the model and computational choices influence joint kinematics, kinetics, and muscle forces resulting from processing the same experimental gait data and (2) to relate the outcome differences to the underlying modeling and computational assumptions.

## Methods

Seven healthy adults (3 females and 4 males, age:  $30.7 \pm 6.1$  years, height:  $176.7 \pm 7.1$  cm, and weight:  $69.4 \pm 6.4$  kg) gave informed consent to participate in the study approved by the Ethics Committee at UZ Leuven (Belgium). Each subject was instrumented with 22 retro-reflective skin-mounted markers, corresponding to the Human Body Model marker set excluding arms, head, and torso<sup>3</sup>. Three-dimensional marker coordinates were recorded (100 Hz) using a ten-camera motion capture system (Vicon, Oxford, UK). Ground Reaction Forces were recorded (1000 Hz) using two force plates (AMTI, Watertown, USA). The subjects were instructed to walk at self-selected speed.

The experimental data were processed with OpenSim 3.3 using the gait2392 model, later referred to as OpenSim model, and with the Gait Offline Analysis Tool 3.3 (Motekforce Link B.V., Amsterdam, The Netherlands) that integrates Human Body Model. The metatarsophalangeal joints of the OpenSim model were locked so that both models had 21 similar DOFs actuated by 43 muscles per leg. Marker information from a standing calibration trial was used to scale the OpenSim model to the subjects' anthropometry using OpenSim's Scale tool (see Tables S1 and S2 in Supplementary Material for the marker pairs used to scale the segments' dimensions and for the marker weights used to fit the model's pose to the standing calibration pose, respectively) and to initialize a new model in Human Body Model<sup>3</sup>.

The processing pipeline with both systems consisted of inverse kinematics, kinematic filtering, inverse dynamics, and static optimization. The same weighted least squares problem (see Table S3 in Supplementary Material for the marker weights) was solved with both systems during inverse kinematics. Details about the different optimization algorithms can be found in Supplementary Material. The resulting root mean square (RMS) and maximum marker errors between modeled and measured marker positions were compared using a Wilcoxon signed rank

statistical analysis. Since OpenSim’s effective dual-pass filter cutoff frequency is lower than the user-specified cutoff frequency<sup>6</sup>, a scaling factor was applied to match Human Body Model’s effective 6 Hz cutoff frequency when filtering the kinematics and the ground reaction forces (more details in Supplementary Material). Human Body Model is real-time and induces a 37 ms time delay when filtering the kinematics<sup>3</sup>. This delay was corrected when comparing the results.

Different static optimization formulations are available in both systems. Human Body Model enables scaling muscle activity by muscle volume in the objective function (default setting)<sup>3,7</sup> whereas OpenSim enables considering the muscles as ideal force generators or constraining them by their force-length-velocity properties<sup>8,9</sup> (more details in Supplementary Material). All formulations were tested to investigate their impact on the muscle force estimation. Similar optimization problems are solved in OpenSim and Human Body Model when the muscles are considered as ideal force generators and when muscle activity is not scaled by muscle volume. However, OpenSim enables the use of reserve actuators whereas Human Body Model does not use upper bounds on muscle activations to guarantee the feasibility of the optimization problem and both systems use different optimization algorithms (more details in Supplementary Material). Both models use identical values for maximal isometric muscle forces to relate muscle activations to muscle forces but there are small differences in moment arms. Human Body Model uses polynomial functions of the joint angles whereas OpenSim uses muscle-tendon paths (line segments between muscle points defined in segmental reference frames) to compute moment arms<sup>3</sup>. Human Body Model’s polynomials are defined such that the moment arms computed based on these polynomials match the OpenSim moment arms within 2 mm for the generic model. Moment arms do not depend on subject size in Human Body Model but are influenced by scaling in OpenSim.

Since the number of gait trials with valid force plate contacts was unevenly divided among subjects, we selected one representative trial for each leg of each subject based on the kinematic errors. We considered each leg apart to increase the size of the dataset. Asymmetry between both legs may exist<sup>10</sup>, contributing to the variability in our data. The representative trial was the trial with the RMS inverse kinematic marker error that best matched the error averaged over all trials<sup>11</sup>. This resulted in 14 trials (stride duration:  $1.05 \pm 0.06$  s) that were used for further analysis. Joint kinematics, kinetics, and muscle forces were time-normalized to the gait cycle duration and averaged over the 14 representative trials. Biomechanical outcomes resulting from the different models and static optimization formulations were analyzed using non-parametric paired t-tests with the one-dimensional statistical parametric mapping package SPM1D<sup>12,13</sup>. The level of significance was set to  $p < .05$ .

To evaluate joint center location differences between models, we calculated the transformations between corresponding segment reference frames that best mapped the OpenSim model markers to the corresponding Human Body Model markers in a least squares sense. We then used these transformations to express the OpenSim model joint centers in the corresponding Human Body Model reference frames and computed the distance between joint centers of both models. To evaluate pelvic reference frame differences, we similarly calculated the transformation between pelvic reference frames and expressed the difference in orientation in Euler angles (sequence of rotation axes: medio-lateral, infero-superior, postero-anterior).

## Results

Differences in joint kinematics were found when processing the same experimental gait data with the OpenSim model and with Human Body Model. Joint kinematics showed similar patterns but statistically differed for all DOFs (maximal statistical differences:  $9.8 \pm 1.5$  degrees,

5.5 ± 1.0 degrees, 8.5 ± 3.6 degrees, 5.0 ± 1.0 degrees, 6.5 ± 1.5 degrees, and 15.6 ± 6.2 degrees for the sagittal hip, frontal hip, transversal hip, sagittal knee, sagittal ankle, and subtalar rotations, respectively) during large intervals ranging from 33 % (sagittal ankle rotation) to 100 % (sagittal hip rotation) of the gait cycle. An offset in sagittal hip rotation (flexion/extension) was observed (Figure 1). After scaling in OpenSim, RMS marker error (1.2 ± 0.1 cm) and maximal marker error (2.2 ± 0.2 cm) of the markers corresponding to anatomical landmarks were close to OpenSim’s recommendations<sup>14</sup> (smaller than 1 and 2 cm, respectively) and had a low sensitivity to user inputs (marker pairs and weights used for scaling) (see Table S4 in Supplementary Material). RMS and maximum marker errors after inverse kinematics were statistically smaller ( $p < .001$ ) with Human Body Model (0.5 ± 0.1 and 1.1 ± 0.3 cm, respectively) than with the OpenSim model (0.7 ± 0.1 and 1.6 ± 0.4 cm, respectively). Marker errors met OpenSim’s best practices<sup>14</sup> (RMS marker error smaller than 2 cm and maximum marker error smaller than 2-4 cm) for both models and had a low sensitivity to user inputs (marker pairs and weights used for scaling and marker weights used for inverse kinematics) in OpenSim (see Table S5 in Supplementary Material).

Differences in joint kinetics were found between the OpenSim model and Human Body Model. Joint moments showed similar patterns but statistically differed during several intervals of the gait cycle for all DOFs (maximal statistical differences: 0.36 ± 0.10 N·m/kg, 0.21 ± 0.03 N·m/kg, 0.09 ± 0.02 N·m/kg, 0.18 ± 0.04 N·m/kg, 0.18 ± 0.03 N·m/kg, and 0.25 ± 0.11 N·m/kg for the sagittal hip, frontal hip, transversal hip, sagittal knee, sagittal ankle, and subtalar moments, respectively) (Figure 2).

Differences in muscle forces were found between the OpenSim model and Human Body Model. Muscle forces computed using similar static optimization formulations showed similar patterns but statistically differed during several intervals of the gait cycle for most muscles (Figure





hip joint center was on average 2.4 cm more anterior in Human Body Model as compared to the OpenSim model. Third, the tibia origins, defining the position of the knee joint centers, had different locations in both models (Table 3). In particular, the tibia origin was on average 1.9 cm more superior in the OpenSim model as compared to Human Body Model. Finally, the subtalar axis was defined differently in both models. The subtalar axes in Human Body Model and in the OpenSim model are inclined by 42 and 37 degrees, respectively, from the transversal plane and deviate medially by -23 and -9 degrees, respectively, from the sagittal plane<sup>16</sup>.

### Discussion

The primary goals of this study were to compare the OpenSim gait2392 model with Human Body Model based on joint kinematics, kinetics, and muscle forces calculated during gait for healthy adults and to relate the outcome differences to the modeling and computational assumptions. Overall, outcome variables had similar patterns across models but they statistically differed in large intervals of the gait cycle.

OpenSim and Human Body Model generate different kinematic models. In particular, we observed large differences in hip and knee joint center locations. Human Body Model estimates the hip joint center locations based on pelvic width and depth using Harrington equations<sup>17</sup>. In OpenSim, the hip joint center locations are scaled with the pelvis. In this study, the hip joint center locations from the generic OpenSim model were scaled in the medio-lateral direction with pelvic width and in the infero-superior and postero-anterior directions with pelvic depth. Kainz *et al*<sup>18</sup> found that Harrington equations are more accurate than other regression equations but suggest the use of functional methods, such as geometric sphere fitting methods<sup>19,20</sup>, in people with sufficient active hip range of motion, as the subjects in this study. More accurate methods to define subject-specific kinematic models<sup>21</sup> have not been integrated in existing software and are not widely

adopted. The OpenSim model and Human Body Model also rely on different joint axis definitions. First, in Human Body Model, the subtalar axis is defined based on the average subtalar joint from Isman and Inman<sup>22</sup> whereas the OpenSim model subtalar axis is derived from Inman<sup>23</sup> and is in the experimental range of values (20 to 68 and -47 to -4 degrees for the horizontal inclination and medial deviation, respectively) obtained from cadaver measurements<sup>22</sup>. Second, the OpenSim model uses a moving knee flexion axis<sup>24</sup> to account for the translation of the tibiofemoral joint in the sagittal plane whereas Human Body Model uses a fixed axis. Finally, there is a large offset between the pelvic reference frames (rotation about the medio-lateral axis) in both models. It is worth mentioning that Roelker *et al.* also reported differences in pelvic neutral position definition between different OpenSim models<sup>4</sup>. This suggests, along with the findings of this study, that this modeling feature is highly variable across existing musculoskeletal models. The differences in pelvic reference frame orientation cause the observed offset in sagittal hip rotation. In combination with the different hip joint center locations, the different pelvic reference frames also explain the different hip rotations in the frontal and transversal planes. The different hip and knee joint center locations and subtalar axis definitions can explain the differences in knee and subtalar rotations. We expect the computational choices (e.g. optimization algorithms and stopping criteria) related to the approaches used for solving inverse kinematics in OpenSim and Human Body Model to have contributed to a lesser extent to the differences in kinematic results than the joint definition differences. Given that OpenSim and Human Body Model use the same initial guesses for the optimization algorithms and that Human Body Model allows a relatively long computational time to solve the inverse kinematic optimization problem, we do not think that convergence to different local optimal or not achieving convergence contributed to the observed differences in kinematics.

The filter used to process the inverse kinematic results has a different order in OpenSim (third order) and in Human Body Model (second order). The users have no access to this computational feature, nor through the graphical user interfaces (GUI) of both software systems, nor through to the application programming interface (API) of OpenSim. We therefore choose to present results obtained with the built-in filters since we expect that most users will perform their entire data processing with either OpenSim or Human Body Model. However, we evaluated the impact of using a second order filter versus a third order filter by processing the OpenSim inverse kinematic results of one trial outside the OpenSim platform before performing inverse dynamics and static optimization. The largest differences in joint moments and muscle forces were 0.06 Nm/kg for the sagittal hip moment and 0.46 N/kg for the rectus femoris, respectively. As a general limitation of this study, due to the limited flexibility of the Human Body Model and OpenSim platforms, we were unable to investigate the influence of each individual modeling and computational choice on the results. As a result, we could only outline important differences in underlying modeling and data processing assumptions without quantifying their relative contributions.

Joint kinematic differences directly affect the joint moments. Other factors also play a role such as different inertial properties<sup>25</sup> and different joint definitions. The different joint definitions will result in different locations and orientations of the joint centers and axes in space after inverse kinematics, and hence the forces and moments applied in the joints to counteract the ground reaction forces and gravity will differ. In particular, we have studied the sensitivity of the joint moments to the knee flexion axis (moving versus fixed) in OpenSim and observed statistical differences (maximal statistical difference:  $0.05 \pm 0.01$  N·m/kg for the knee) (Figure S13 in Supplementary Material).

Differences in muscle forces result from differences in joint kinematics and kinetics as well as from differences in moment arms. These differences in moment arms are due to the different computation of moment arms in both models, to the different joint kinematics that are inputs to this computation, and to the influence of the subject size that is taken into account in OpenSim but not in Human Body Model. Differences in joint kinematics between the OpenSim model and Human Body Model induced differences in moment arms up to 1.5 cm (quadratus femoris for hip flexion). Differences in moment arms between the smallest (height: 169 cm) and the tallest (height: 190 cm) subjects were up to 0.9 cm (gluteus maximus 3 (posterior part) for hip flexion) in the anatomical position. In Human Body Model, psoas muscle activations exceeded one suggesting an unrealistic muscle force distribution. It was more optimal to activate the psoas above one than increasing the contribution of another muscle (e.g. rectus femoris). Muscle activations exceeding one were dependent on the static optimization objective function. In more detail, piriformis muscle activations exceeded one (maximum 1.1) for two out of 14 trials during small intervals of the gait cycle (<7 %) when scaling muscle activity by muscle volume in the static optimization objective function. This underlines the importance of the criterion used to solve the muscle redundancy problem. However, it is to be mentioned that muscle activations will also depend on the muscle-tendon parameters, which appear in the objective function. We expect that more representative muscle-tendon parameters will result in muscle activations smaller than one during gait for both objective functions. Overall, activations larger than one are not physiological and should be identified as a limitation of the model. Finally, no experimental muscle activations (electromyography) were available to further validate the static optimization results, which is a limitation of this study.

Modeling assumptions affect the estimation of muscle forces. In particular, the sensitivity of the results to the choice of the objective function was underlined by the differences observed in estimated muscle forces when scaling muscle activity by muscle volume in the static optimization objective function in Human Body Model. Constraining the muscles by their force-length-velocity properties in OpenSim had less influence on the estimated muscle forces. However, this constraint might be more important for faster motions for which muscle properties and dynamics play a more important role<sup>26,27</sup>. Finally, for various reasons, we expect different optimization algorithms and stopping criteria in OpenSim and Human Body Model to have a limited influence on the static optimization results. First, we have studied the sensitivity of the results to the stopping criteria in OpenSim and found that muscle activations differed at most by  $1e-4$  (biceps femoris short head) when changing the convergence criterion (from  $1e-4$  to  $1e-5$ ) and the maximum number of iterations (from 100 to 10,000). Second, Human Body Model allows a relatively long computational time to solve the static optimization problem, limiting the risks of sub-optimal solutions. Third, the static optimization problem is a quadratic programming problem (i.e. local optima are global optima) and the initial guesses will therefore not affect the results.

OpenSim and Human Body Model were designed with different applications and target users in mind. Human Body Model is real-time and aimed towards clinicians with no particular technical skills. It relies on a pre-defined muscle model which may not be suitable when subject-specificity is required<sup>28,29</sup>. OpenSim is open-source, enables subject-specific modeling, and is more aimed towards researchers with technical background. Its standard workflow is offline although an OpenSim-based real-time system was recently developed to compute inverse kinematics and inverse dynamics for lower-limb applications<sup>30</sup>. Finally, Human Body Model does not require user inputs to create a model and is therefore robust against user errors. In contrast,

OpenSim provides the users with more flexibility in the scaling and inverse kinematic setups. However, the user choices can have an influence on the results (see Table S5 in Supplementary Material).

We found differences in joint kinematics, kinetics, and muscle forces resulting from processing the same experimental gait data from healthy adults using the OpenSim model and Human Body Model. Both models are similar in many aspects but differ in the definitions of the kinematic model (joint center and axis definitions) and we expect these differences to be the main causes for the outcome differences. Since different computational choices resulted in different muscle forces, continued efforts for validating models and methods are required<sup>15,31</sup>. Depending on the aim, differences in biomechanical variables between models and software systems may be more or less important. In clinical analyses, focus is on interpreting deviations from reference data. Processing reference and patient data with the same model and software system is hence in general sufficient to deal with model and computational uncertainties. We compared standard deviations of joint kinematics and kinetics between the OpenSim model and Human Body Model as well as which trials deviated more than one standard deviation from the mean (see Table S6 in Supplementary Material). Since we observed similar results, we expect similar interpretations when comparing reference and patient data based on either the OpenSim model or Human Body Model. In contrast, as described by Roelker *et al.*<sup>4</sup>, processing reference and patient data with different models and software systems may result in incorrect interpretations if discrepancies between models and software systems are not taken into account. In mechanical analyses, the goal is to obtain accurate estimates of kinematics and loading and, therefore, discrepancies between models or computational choices may lead to different conclusions. In such cases, musculoskeletal models should be used with care. Similarly, differences in biomechanical variables are important

when comparing results from studies in the literature that were obtained with different models and software systems. Differences that are smaller than the differences reported in this study cannot be attributed to differences in the movement execution.

Based on the results of this study, we recommend researchers aiming to compare their results with results from other simulation studies to pay special attention to the definition of the pelvic reference frame, the hip and knee joint centers, and the static optimization cost function. Since it is currently unknown which cost function provides the ‘best’ approximation of the human control strategy, computed muscle activations should be interpreted carefully and, whenever possible, compared to experimentally measured muscle activations. Muscle forces are the main determinants of lower limb contact forces during walking. The large differences in muscle forces might therefore influence the evaluation of joint loading. We previously found differences in knee joint loading of about 8 N/kg between healthy individuals and patients with severe osteoarthritis<sup>32</sup>. Similar differences might be caused by the differences in magnitudes of the muscle forces we report here. However, all muscles spanning a joint determine joint loading and therefore additional model comparison is needed to evaluate the effect of model choice on joint loading. Nevertheless, we advise researchers to be aware of the effect of modelling choices on computed muscle forces when evaluating joint loading. Overall, in model-based biomechanical analyses, users should be conscious of the modeling and computational assumptions and their influence on the biomechanical variables.

### **Acknowledgments**

Research funded by a Ph.D. grant (1S35416N) of the Research Foundation Flanders (FWO).



## References

1. Damsgaard M, Rasmussen J, Christensen ST, Surma E, de Zee M. Analysis of musculoskeletal systems in the AnyBody Modeling System. *Simul Model Pr Th*. 2006;14(8):1100-1111.
2. Delp SL, Anderson FC, Arnold AS, et al. OpenSim: open-source software to create and analyze dynamic simulations of movement. *IEEE T Biomed Eng*. 2007;54(11):1940-1950.
3. van den Bogert AJ, Geijtenbeek T, Even-Zohar O, Steenbrink F, Hardin EC. A real-time system for biomechanical analysis of human movement and muscle function. *Med Biol Eng Comput*. 2013;51(10):1069-1077.
4. Roelker SA, Caruthers EJ, Baker RK, Pelz NC, Chaudhari AMW, Siston RA. Interpreting musculoskeletal models and dynamic simulations: causes and effects of differences between models. *Ann Biomed Eng*. 2017;45(11):2635-2647.
5. Delp SL, Loan P, Hoy MG, Zajac FE, Topp EL, Rosen JM. An interactive graphics-based model of the lower extremity to study orthopaedic surgical procedures. *IEEE T Biomed Eng*. 1990;37(8):757-767.
6. Winter DA. *Biomechanics and Motor Control of Human Movement*. 4th ed. Hoboken, New Jersey: John Wiley & Sons, Inc.; 2009.
7. Holmberg JL, Klarbring A. Muscle decomposition and recruitment criteria influence muscle force estimates. *Multibody Syst Dyn*. 2012;28(3):283-289.
8. Zajac FE. Muscle and tendon: properties, models, scaling, and application to biomechanics and motor control. *Crit Rev Biomed Eng*. 1989;17(4):359-411.
9. Crowninshield RD, Brand RA. A physiologically based criterion of muscle force prediction in locomotion. *J Biomech*. 1981;14(11):793-801.
10. Lathrop-Lambach RL, Asay JL, Jamison ST, et al. Evidence for joint moment asymmetry in healthy populations during gait. *Gait Posture*. 2014;40(4):526-531.
11. Dixon PC, Stebbins J, Theologis T, Zavatsky AB. Spatio-temporal parameters and lower-limb kinematics of turning gait in typically developing children. *Gait Posture*. 2013;38(4):870-875.
12. Pataky TC, Robinson MA, Vanrenterghem J. Vector field statistical analysis of kinematic and force trajectories. *J Biomech*. 2013;46(14):2394-2401.
13. Nichols TE, Holmes AP. Nonparametric permutation tests for functional neuroimaging: A primer with examples. *Hum Brain Mapp*. 2002;15(1):1-25.
14. Hicks JL, Seth A, Hamner SR, et al. Simulation with OpenSim - Best Practices. <https://simtk-confluence.stanford.edu/display/OpenSim/Simulation+with+OpenSim++Best+Practices>.

15. Hicks JL, Uchida TK, Seth A, Rajagopal A, Delp SL. Is my model good enough? Best practices for verification and validation of musculoskeletal models and simulations of human movement. *J Biomech Eng.* 2015;137(2):020905:1-020905:24.
16. Delp SL. Surgery simulation: a computer graphics system to analyze and design musculoskeletal reconstructions of the lower limb. 1990.
17. Harrington ME, Zavatsky AB, Lawson SEM, Yuan Z, Theologis TN. Prediction of the hip joint centre in adults, children, and patients with cerebral palsy based on magnetic resonance imaging. *J Biomech.* 2007;40(3):595-602.
18. Kainz H, Carty CP, Modenese L, Boyd RN, Lloyd DG. Estimation of the hip joint centre in human motion analysis: A systematic review. *Clin Biomech.* 2015;30(4):319-329.
19. Piazza SJ, Okita N, Cavanagh PR. Accuracy of the functional method of hip joint center location : effects of limited motion and varied implementation. *J Biomech.* 2001;34(7):967-973.
20. Besier TF, Sturnieks DL, Alderson JA, Lloyd DG. Repeatability of gait data using a functional hip joint centre and a mean helical knee axis. *J Biomech.* 2003;36(8):1159-1168.
21. Reinbolt JA, Schutte JF, Fregly BJ, et al. Determination of patient-specific multi-joint kinematic models through two-level optimization. *J Biomech.* 2005;38(3):621-626.
22. Isman RE, Inman VT. Anthropometric Studies of the Human Foot and Ankle. *Foot Ankle.* 1969;11:97-129.
23. Inman VT. *The Joints of the Ankle.* Baltimore: Williams & Wilkins; 1976.
24. Yamaguchi GT, Zajac FE. A planar model of the knee joint to characterize the knee extensor mechanism. *J Biomech.* 1989;22(1):1-10.
25. Wesseling M, de Groote F, Jonkers I. The effect of perturbing body segment parameters on calculated joint moments and muscle forces during gait. *J Biomech.* 2014;47(2):596-601.
26. De Groote F, Kinney AL, Rao AV, Fregly BJ. Evaluation of direct collocation optimal control problem formulations for solving the muscle redundancy problem. *Ann Biomed Eng.* 2016;44(10):2922-2936.
27. Miller RH, Umberger BR, Caldwell GE. Limitations to maximum sprinting speed imposed by muscle mechanical properties. *J Biomech.* 2012;45(6):1092-1097.
28. Fregly BJ, Boninger ML, Reinkensmeyer DJ. Personalized neuromusculoskeletal modeling to improve treatment of mobility impairments: a perspective from European research sites. *J Neuroeng Rehabil.* 2012;9(1):18.
29. Falisse A, Van Rossom S, Jonkers I, De Groote F. EMG-driven optimal estimation of subject-specific Hill model muscle-tendon parameters of the knee joint actuators. *IEEE T Biomed Eng.* 2017;64(9):2253-2262.



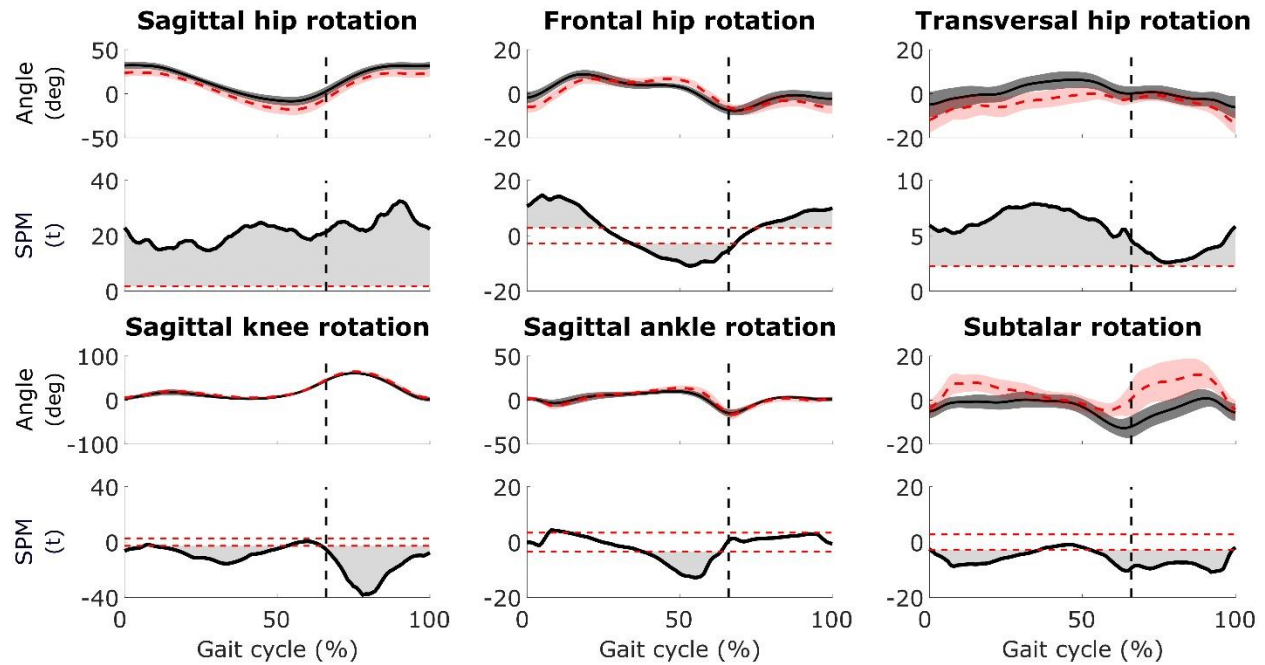


**Figure 1** – [First and third row] Comparison of joint kinematics calculated with the OpenSim model (dashed red) and Human Body Model (black). [Second and fourth row] Results from the statistical analysis using non-parametric paired t-tests in SPM1D. Grey shaded areas above and below the red dashed lines indicate significant differences. The vertical black dashed line indicates the transition from stance to swing.

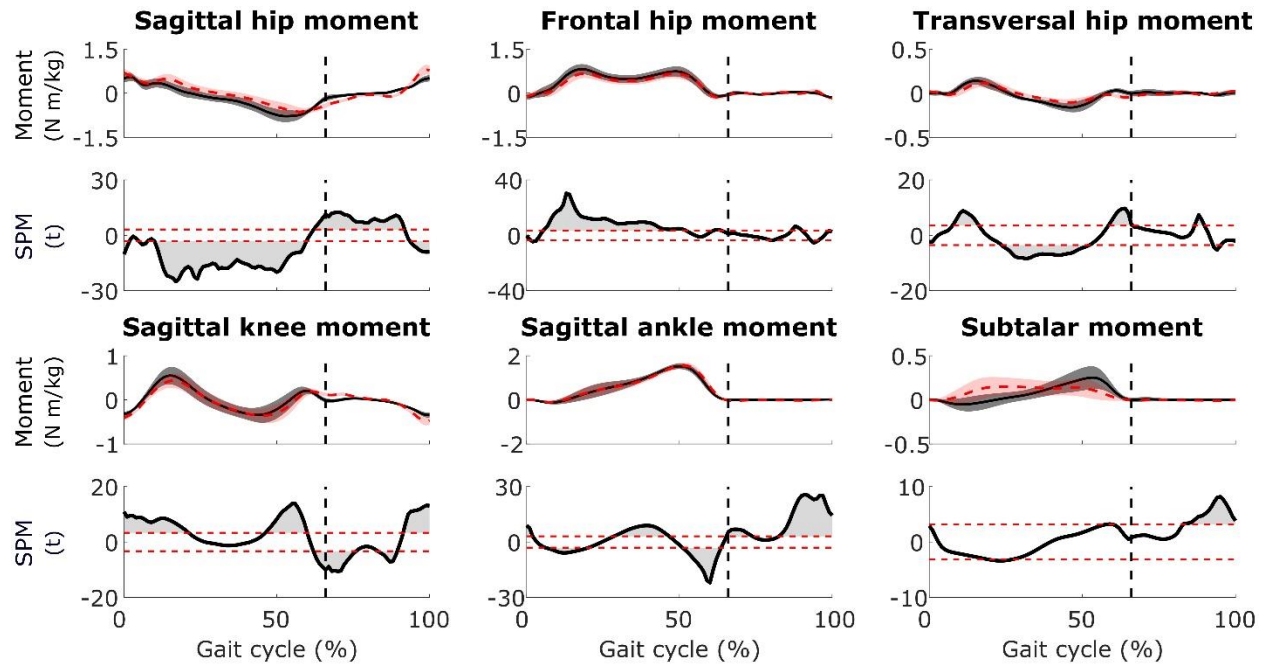


**Figure 2** – [First and third row] Comparison of joint kinetics calculated with the OpenSim model (dashed red) and Human Body Model (black). [Second and fourth row] Results from the statistical analysis using non-parametric paired t-tests in SPM1D. Grey shaded areas above and below the red dashed lines indicate significant differences. The vertical black dashed line indicates the transition from stance to swing.

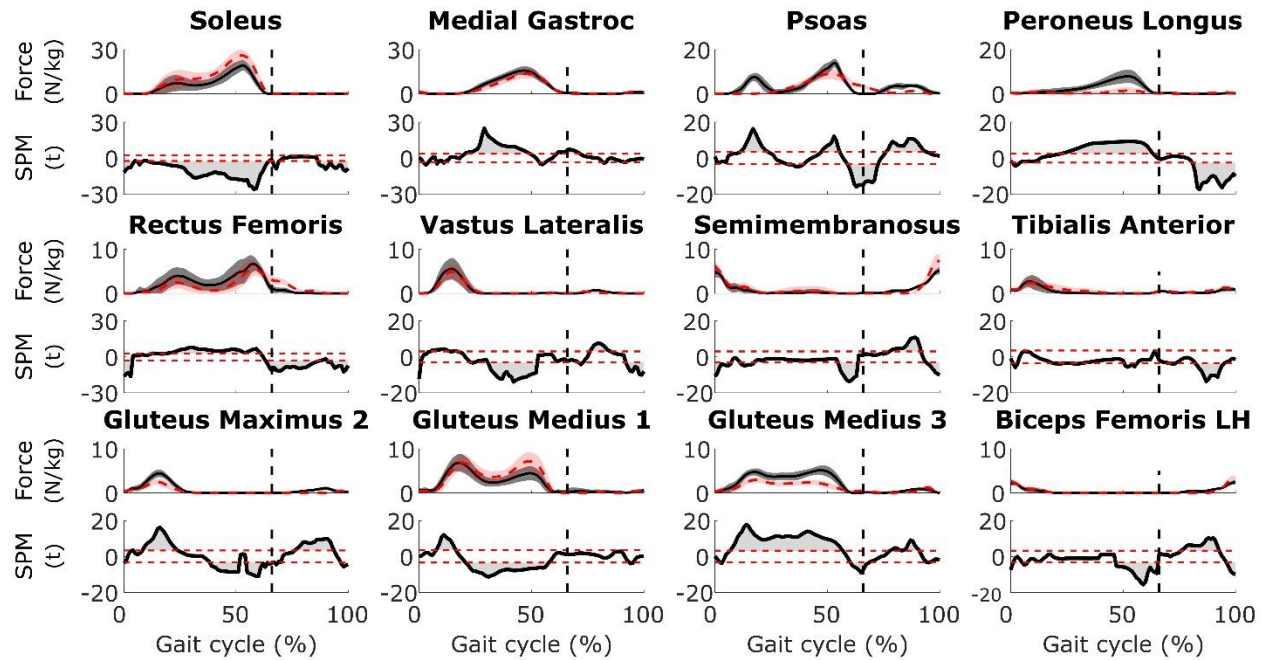


**Figure 3** – [First, third, and fifth row] Comparison of muscle forces estimated with the OpenSim model (dashed red) and Human Body Model (black). Muscle forces estimated without taking force-length-velocity properties into account (OpenSim) and without scaling muscle activity by muscle volume in the static optimization objective function (Human Body Model). [Second, fourth, and sixth row] Results from the statistical analysis using non-parametric paired t-tests in SPM1D. Grey shaded areas above and below the red dashed lines indicate significant differences. The vertical black dashed line indicates the transition from stance to swing. See Figures S1-4 in Supplementary Material for other muscles.

**Table 1:** Differences in pelvic reference frame orientation between OpenSim model and Human Body Model evaluated through Euler angles (degree).

Rotation axes	Subjects							mean ± std
	1	2	3	4	5	6	7	
<b>Medio-lateral</b>	10.1	10.3	10.5	10.8	9.2	9.3	11.1	<b>10.2 ± 0.7</b>
<b>Infero-superior</b>	-1.1	0.8	0.1	-0.3	1.0	-0.4	-2.3	<b>-0.3 ± 1.1</b>
<b>Postero-anterior</b>	-0.6	-1.0	1.3	-0.3	0.2	-1.4	-0.2	<b>-0.3 ± 0.9</b>

*Note:* Euler angles in degree, sequence of rotation axes: medio-lateral, infero-superior, postero-anterior, describing the orientation of the pelvic reference frame of the OpenSim model with respect to the pelvic reference frame of Human Body Model.

**Table 2:** Differences (cm) in right hip joint center location between OpenSim model and Human Body Model

Axes	Subjects							mean ± std
	1	2	3	4	5	6	7	
<b>Postero-anterior</b>	2.2	2.3	2.5	1.9	2.9	2.7	2.5	<b>2.4 ± 0.3</b>
<b>Infero-superior</b>	1.2	1.6	1.0	0.6	1.4	1.7	2.8	<b>1.5 ± 0.7</b>
<b>Medio-lateral</b>	1.0	0.7	1.3	0.9	0.8	0.8	1.5	<b>1.0 ± 0.3</b>

*Note:* differences in cm between Human Body Model right hip joint center location and the OpenSim model right hip joint center location expressed in Human Body Model pelvic reference frame. Positive results indicate a more anterior/superior/lateral location in Human Body Model as compared to the OpenSim model.







where  $n$  is the order of the filter. To match the 6 Hz cutoff frequency used in the Human Body Model real-time filter to process the joint kinematics, we therefore selected a  $6.9494 = 6/0.8634$  Hz cutoff frequency in OpenSim where 0.8634 is the scaling factor obtained from equation 1 with  $n = 3$ .

Human Body Model also processes the ground reaction forces using the same real-time filter. This step is not part of the standard OpenSim data processing pipeline and was therefore performed manually using a second-order zero-phase forward and reverse low-pass Butterworth filter. The order of the filter was chosen to match the one used in Human Body Model and a  $7.4790 = 6/0.8022$  Hz cutoff frequency (where 0.8022 is the scaling factor obtained from equation 1 with  $n = 2$ ) was selected to compensate for the dual-pass. The ground reaction forces were therefore processed in a similar way with both models / software systems.

### Inverse kinematics

Table S3 gives the marker weights used during inverse kinematics in OpenSim and Human Body Model. We have investigated the sensitivity of the inverse kinematic results to the set of marker weights in OpenSim. In particular, we have compared two sets of marker weights ( $S_a$  and  $S_b$  in Table S3). The first set of marker weights ( $S_a$ ) was used to generate the results of this study. The results of the sensitivity analysis are presented in Table S5.

OpenSim solves the inverse kinematic problem using a general quadratic programming solver, with a convergence criterion of  $1e-4$  and a limit of 1000 iterations per frame. For unconstrained problems with bounded coordinates, the LBFGS method<sup>2</sup> is used as optimization algorithm. Human Body Model solves the inverse kinematic problem using the Levenberg-Marquardt algorithm<sup>3</sup> with a limit of 99 iterations and 0.99 s per frame, and a tolerance level of  $1e-4$ . These stopping criteria are for non-real time, using the Gait Offline Analysis Tool. Both

algorithms use as initial guess the model in the default position for the first frame and then, for each frame, the solution from the previous frame.

### Static optimization

A static optimization problem was solved to estimate the muscle forces<sup>4</sup>. Different formulations of the optimization problem are available in both systems.

In Human Body Model, two objective functions  $J1$  (equation 2) and  $J2$  (equation 3) can be selected. They differ by a scaling factor introduced in  $J2$  that weights the squared normalized muscle forces by the muscle volume. The mathematical expressions of these objective functions are given by:

$$J1 = \sum_{i=1}^m \left( \frac{F_i}{F_{max,i}} \right)^2, \quad (2)$$

where  $m$  is the number of muscles,  $i$  is the muscle index,  $F$  is the muscle force, and  $F_{max}$  is the maximal isometric muscle force, and:

$$J2 = \sum_{i=1}^m V_i \left( \frac{F_i}{F_{max,i}} \right)^2, \quad (3)$$

where  $V$  is proportional to muscle volume ( $V = l^{opt} F_{max}$  where  $l^{opt}$  is the optimal muscle fiber length).

In OpenSim, the muscles can be considered as ideal force generators or constrained by their force-length-velocity properties<sup>5</sup>. The objective function  $J3$  used in OpenSim is given by:

$$J3 = \sum_{i=1}^m (a_i)^2, \quad (4)$$

where  $a$  is the muscle activation.

When considering the muscles as ideal force generators (by not taking into account force-length-velocity properties of muscle),  $J3$  equals  $J1$  since  $a = F/F_{max}$ , and the formulation of the static optimization problem is therefore similar in OpenSim and Human Body Model. The comparison of the muscle forces estimated based on this formulation in OpenSim and Human Body Model is presented in Figures S1-4. The impact of the force-length-velocity properties on the muscle forces estimated in OpenSim is presented in Figures S5-8. Finally, the impact of the muscle volume scaling (equation 3) on the muscle forces estimated in Human Body Model is presented in Figures S9-12. Note that the tendon is assumed to be rigid in static optimization.

OpenSim solves the static optimization problem using the interior-point algorithm IPOPT<sup>6</sup>, with a converge criterion of  $1e-4$  and a limit of 100 iterations per frame. Human Body Model solves the static optimization problem using a recurrent neural network<sup>7</sup>, simulated numerically with the forward Euler method<sup>8</sup>, with a limit of 10,000 iterations and 0.05 s per frame, and a tolerance level of  $1e-2$ . These stopping criteria are for non-real time, using the Gait Offline Analysis Tool.

## References

1. Winter DA. *Biomechanics and Motor Control of Human Movement*. 4th ed. Hoboken, New Jersey: John Wiley & Sons, Inc.; 2009.
2. Byrd RH, Lu P, Nocedal J, Zhu C. A limited memory algorithm for bound constrained optimization. *J SCI Comput*. 1995;16(5):1190–1208.
3. Press WH, Teukolsky SA, Vetterling WT, Flannery BP. *Numerical Recipes. The Art of Scientific Computing*. 3rd ed. Cambridge: Cambridge University Press; 2007.
4. Crowninshield RD, Brand RA. A physiologically based criterion of muscle force prediction in locomotion. *J Biomech*. 1981;14(11):793-801.
5. Zajac FE. Muscle and tendon: properties, models, scaling, and application to biomechanics and motor control. *Crit Rev Biomed Eng*. 1989;17(4):359-411.
6. Wächter A, Biegler LT. On the implementation of an interior-point filter line-search algorithm for large-scale nonlinear programming. *Math Progr*. 2006;106(1):25-57.
7. Xia Y, Feng G. An improved neural network for convex quadratic optimization with application to real-time beamforming. *Neurocomputing*. 2005;64:359-374.
8. van den Bogert AJ, Geijtenbeek T, Even-Zohar O, Steenbrink F, Hardin EC. A real-time system for biomechanical analysis of human movement and muscle function. *Med Biol Eng Comput*. 2013;51(10):1069-1077.

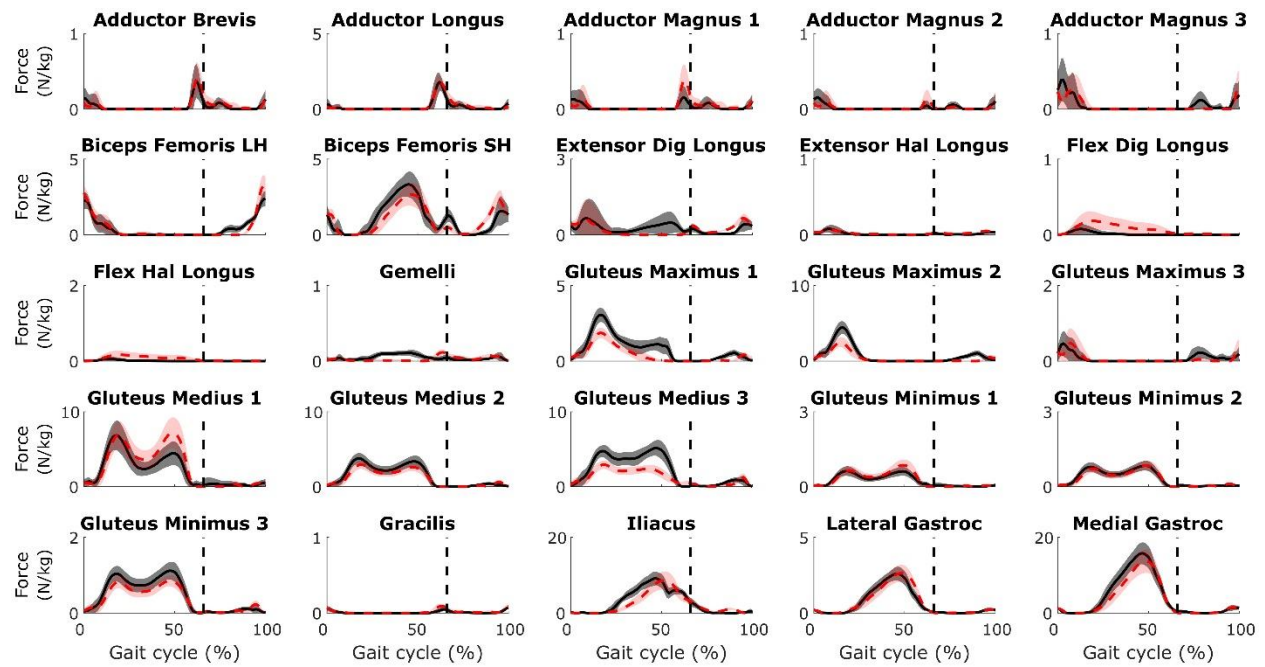


**Figure S1** – Comparison of muscle forces estimated with the OpenSim gait2392 model (dashed red) and Human Body Model (black). Muscle forces estimated considering the muscles as ideal force generators (OpenSim) and without scaling the static optimization objective function by muscle volume (Human Body Model). The vertical black dashed line indicates the transition from stance to swing – Part 1

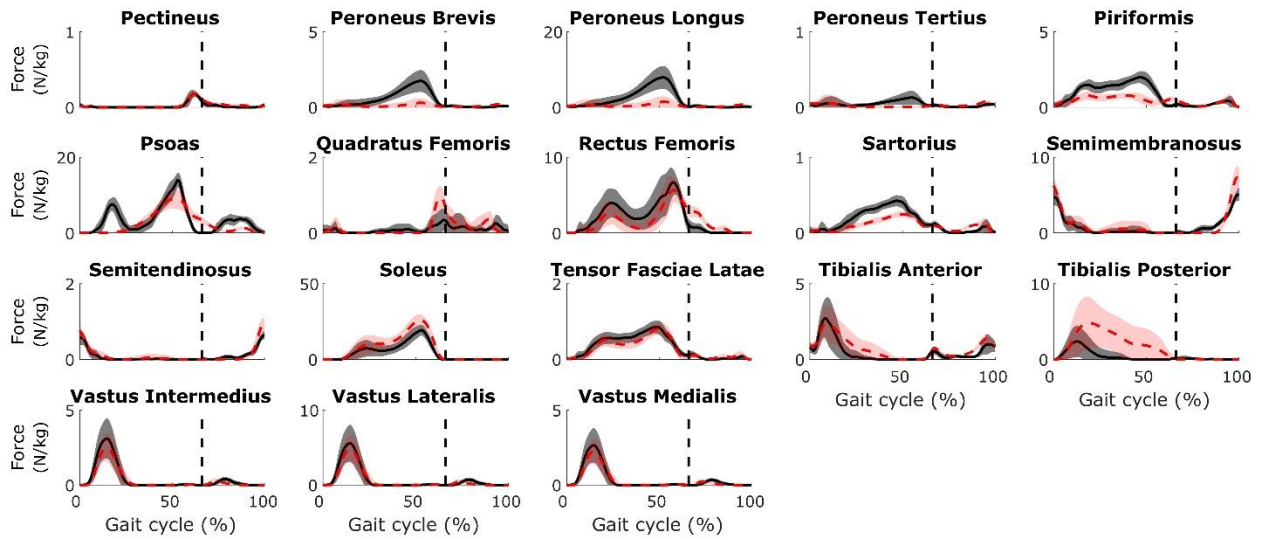


**Figure S2** – Comparison of muscle forces estimated with the OpenSim gait2392 model (dashed red) and Human Body Model (black). Muscle forces estimated considering the muscles as ideal force generators (OpenSim) and without scaling the static optimization objective function by muscle volume (Human Body Model). The vertical black dashed line indicates the transition from stance to swing – Part 2

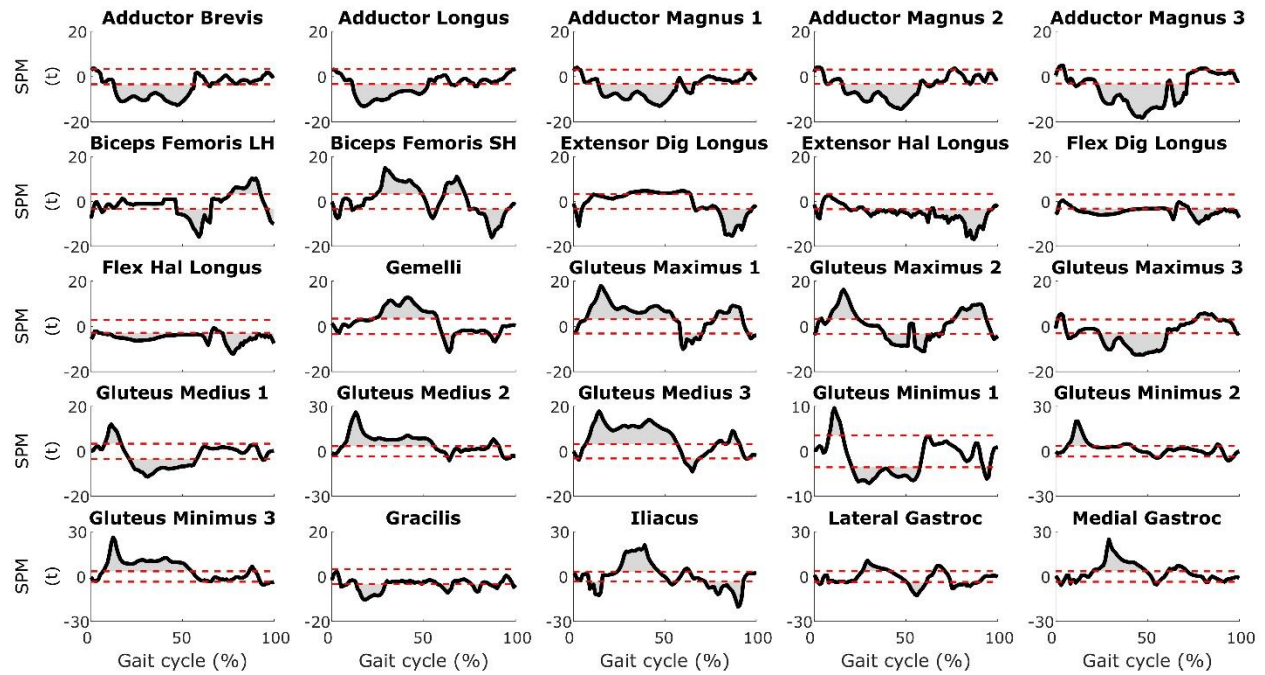


**Figure S3** – Results from the statistical analysis comparing muscle forces estimated with the OpenSim gait2392 model and Human Body Model (see Figure S1) using non-parametric paired t-tests in SPM1D. Grey shaded areas above and below the red dashed lines indicate significant differences – Part 1



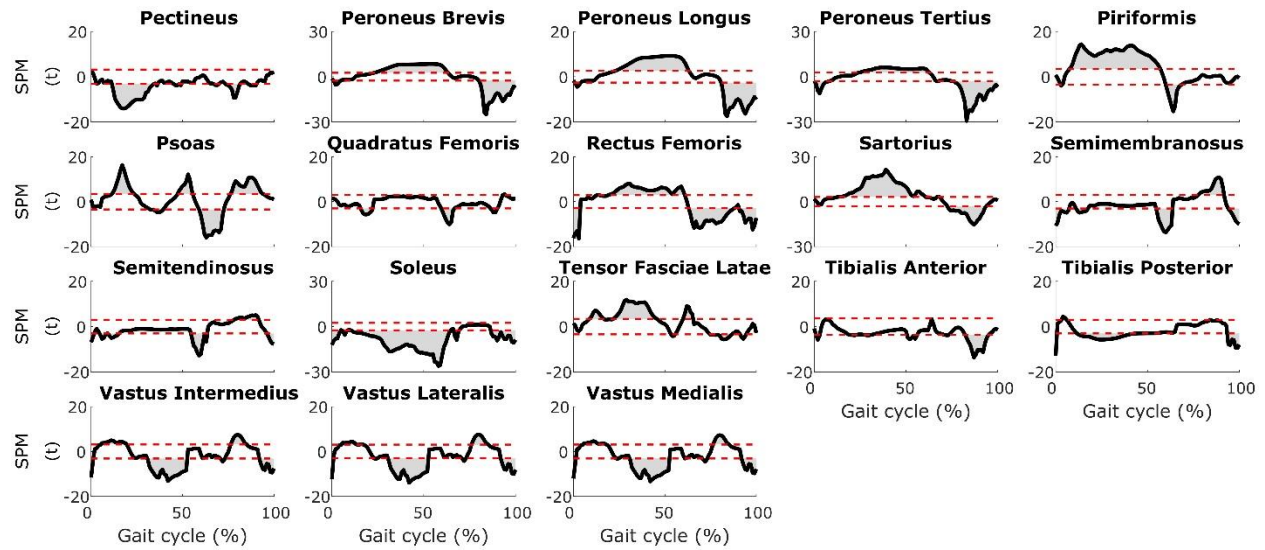


**Figure S4** – Results from the statistical analysis comparing muscle forces estimated with the OpenSim gait2392 model and Human Body Model (see Figure S2) using non-parametric paired t-tests in SPM1D. Grey shaded areas above and below the red dashed lines indicate significant differences - Part 2

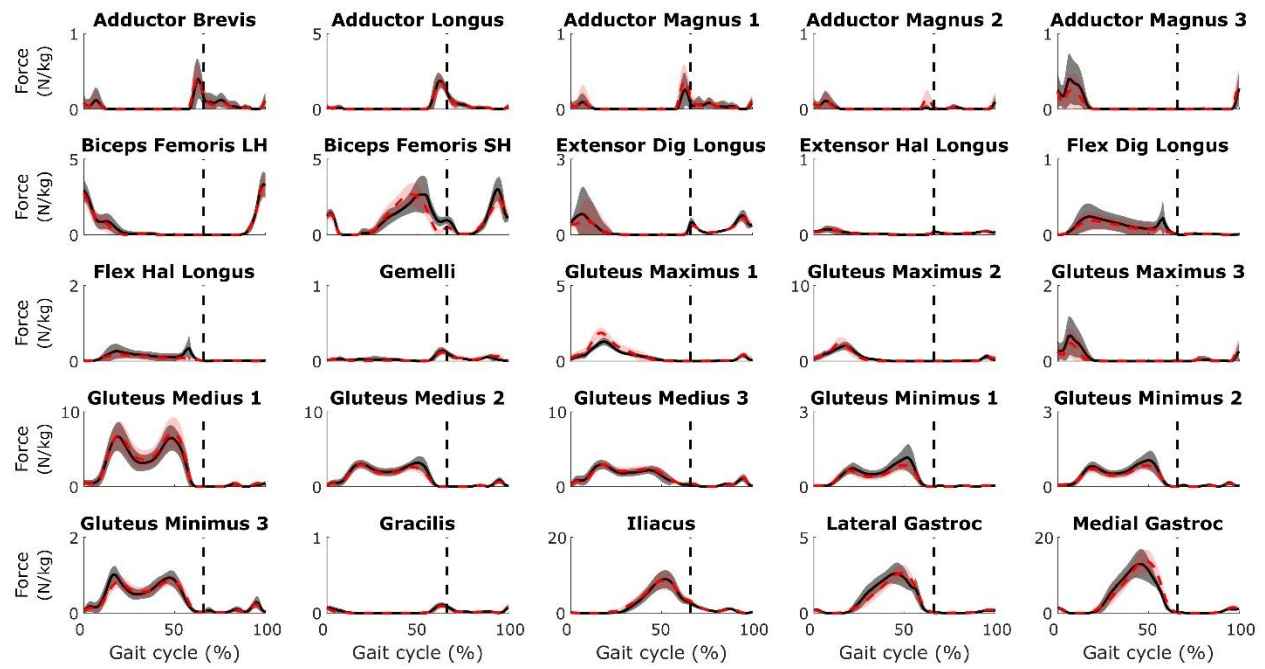


**Figure S5** – Comparison of muscle forces estimated with the OpenSim gait2392 model considering the muscles as ideal force generators (dashed red) or taking the force-length-velocity properties into account (black). The vertical black dashed line indicates the transition from stance to swing - Part 1

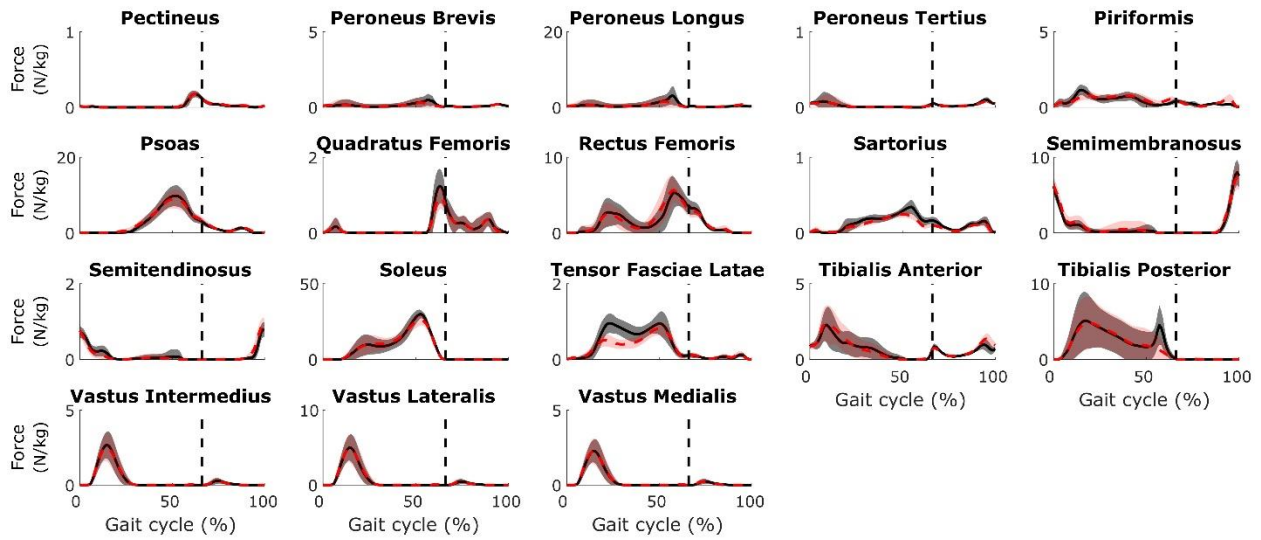


**Figure S6** – Comparison of muscle forces estimated with the OpenSim gait2392 model considering the muscles as ideal force generators (dashed red) or taking the force-length-velocity properties into account (black). The vertical black dashed line indicates the transition from stance to swing - Part 2

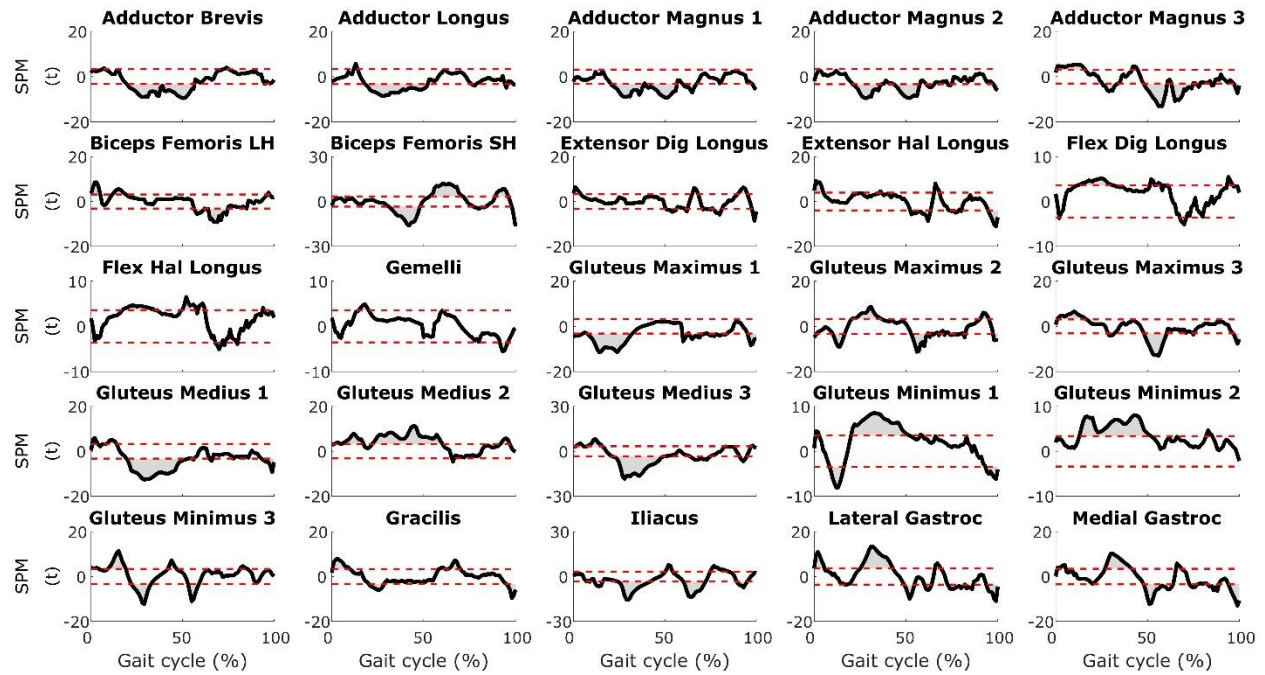


**Figure S7** – Results from the statistical analysis comparing muscle forces estimated with the OpenSim gait2392 model considering the muscles as ideal force generators or taking the force-length-velocity properties into account (see Figure S5) using non-parametric paired t-tests in SPM1D. Grey shaded areas above and below the red dashed lines indicate significant differences - Part 1

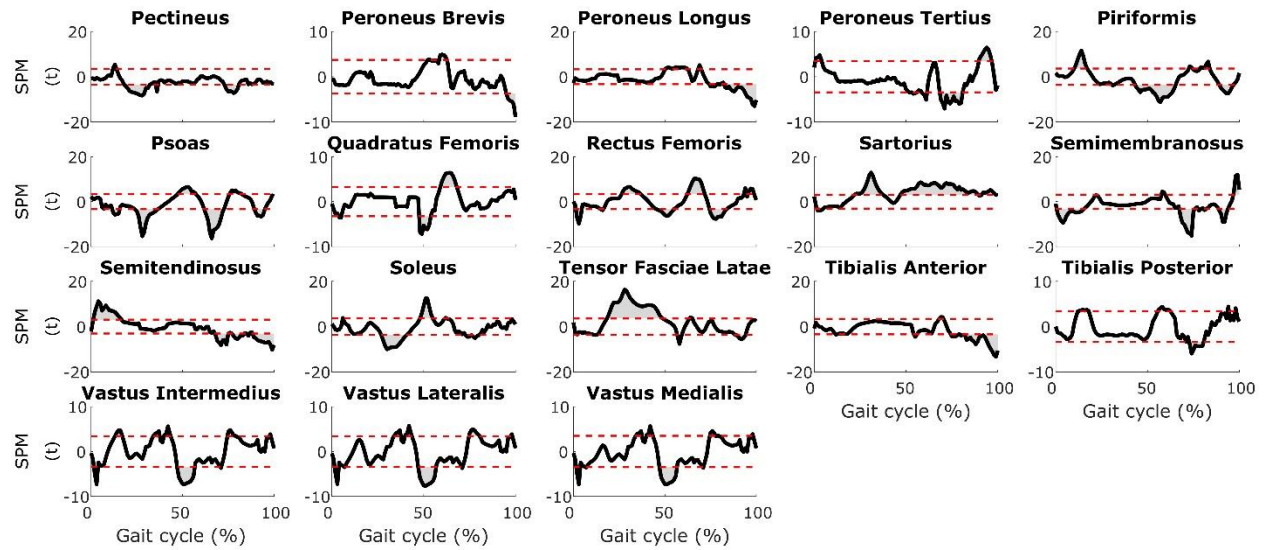


**Figure S8** – Results from the statistical analysis comparing muscle forces estimated with the OpenSim gait2392 model considering the muscles as ideal force generators or taking the force-length-velocity properties into account (see Figure S6) using non-parametric paired t-tests in SPM1D. Grey shaded areas above and below the red dashed lines indicate significant differences - Part 2

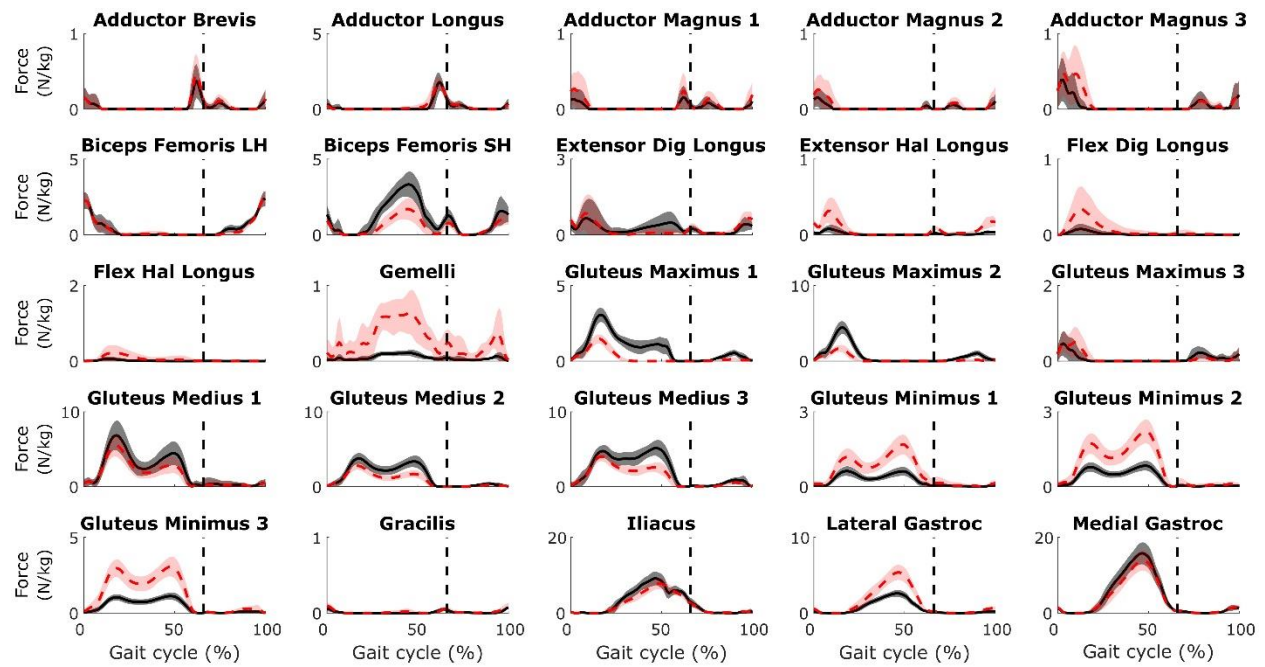


**Figure S9** – Comparison of muscle forces estimated in Human Body Model with (dashed red) and without (black) scaling the static optimization objective function by muscle volume. The vertical black dashed line indicates the transition from stance to swing - Part 1

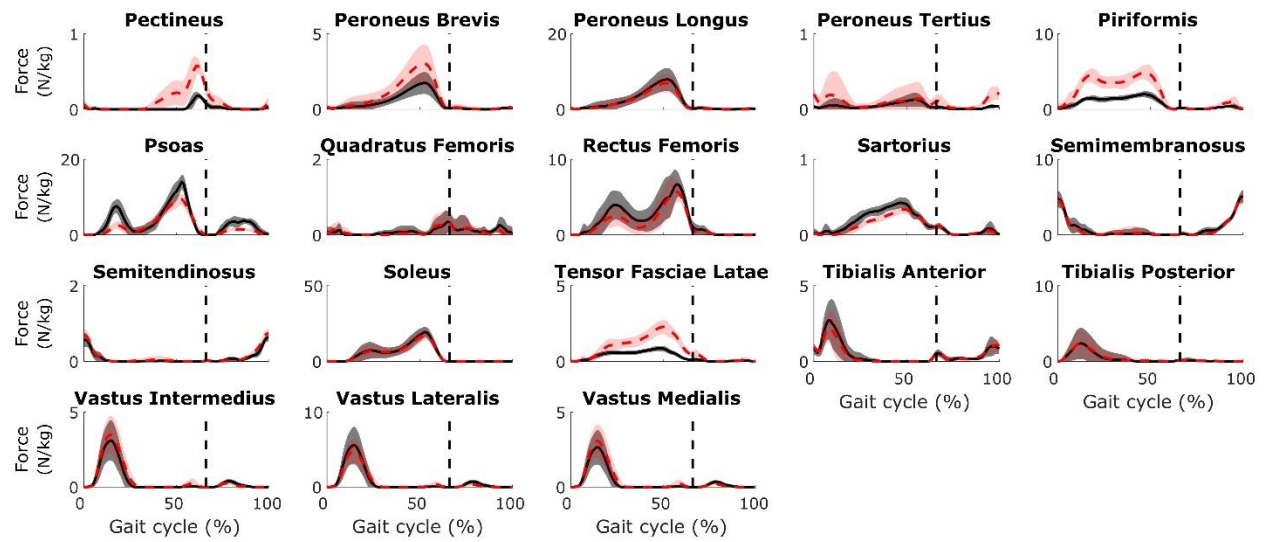


**Figure S10** – Comparison of muscle forces estimated in Human Body Model with (dashed red) and without (black) scaling the static optimization objective function by muscle volume. The vertical black dashed line indicates the transition from stance to swing - Part 2

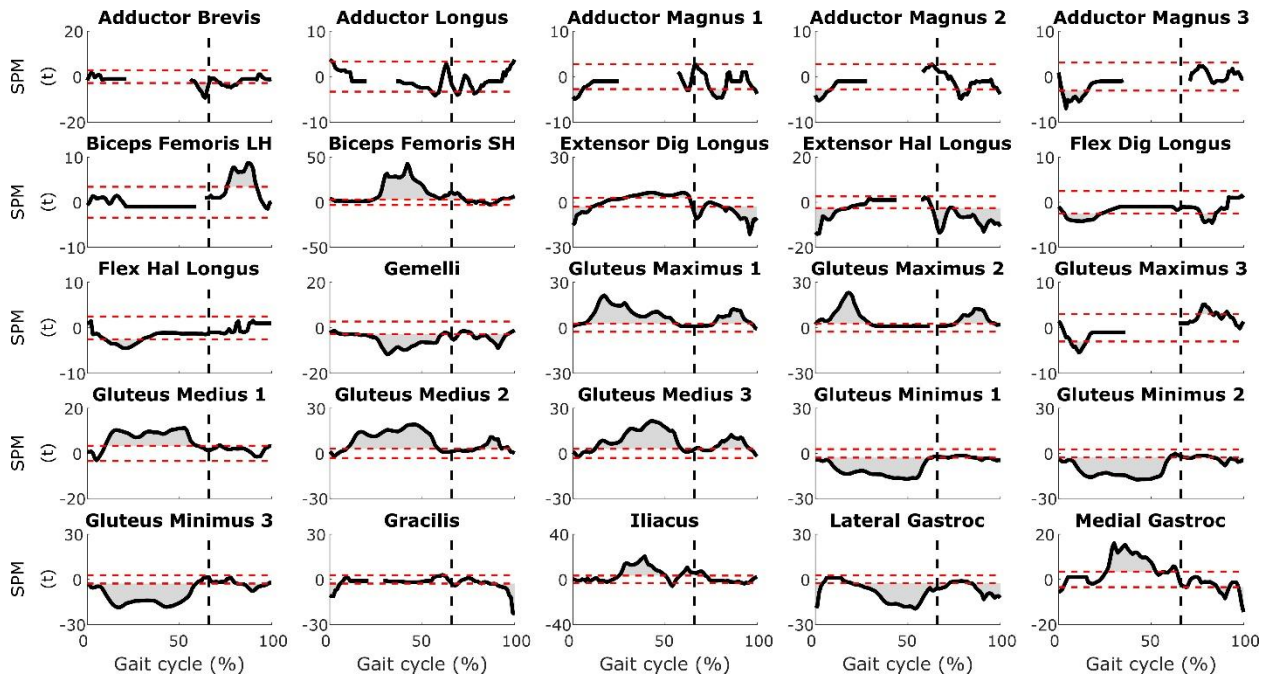


**Figure S11** – Results from the statistical analysis comparing muscle forces estimated in Human Body Model with and without scaling the static optimization objective function by muscle volume (see Figure S9) using non-parametric paired t-tests in SPM1D. Grey shaded areas above and below the red dashed lines indicate significant differences. Parts without t waveforms were excluded from the analysis since there was no variance - Part 1



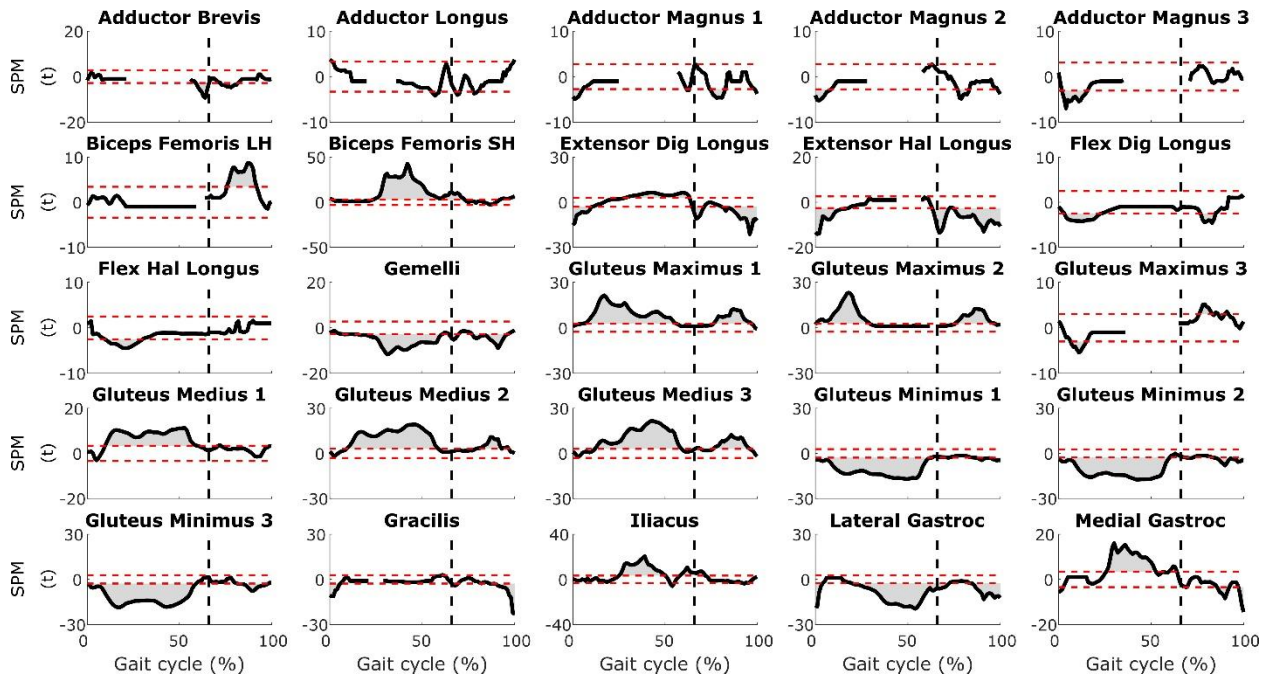


**Figure S12** – Results from the statistical analysis comparing muscle forces estimated in Human Body Model with and without scaling the static optimization objective function by muscle volume (see Figure S10) using non-parametric paired t-tests in SPM1D. Grey shaded areas above and below the red dashed lines indicate significant differences. Parts without t waveforms were excluded from the analysis since there was no variance - Part 2



**Table S1:** Marker pairs used during scaling in OpenSim.

Body	Marker pair 1		Marker pair 2		Marker pair 3		Marker pair 4	
<b>Pelvis (medio-lateral)</b>	R ASIS	L ASIS						
<b>Pelvis (postero-anterior)</b>	R ASIS	R PSIS	L ASIS	L PSIS				
<b>Pelvis (infero-superior)</b>	R ASIS	R PSIS	L ASIS	L PSIS				
<b>Femur</b>	R ASIS	R MEK	L ASIS	L MEK	R ASIS	R LEK	L ASIS	L LEK
<b>Tibia</b>	R MEK	R MM	L MEK	L MM	R LEK	R LM	L LEK	L LM
<b>Foot</b>	R HEE	R MT2	L HEE	L MT2				

*Note:* R-L are for Right-Left, ASIS is for anterior superior iliac spine, PSIS is for posterior superior iliac spine, MEK is for medial epicondyle of the knee, LEK is for lateral epicondyle of the knee, MM is for medial malleolus, LM is for lateral malleolus, HEE is for heel, and MT2 is for second meta tarsal.

**Table S2:** Marker weights used during scaling in OpenSim.

Marker	Weight		Marker	Weight		Marker	Weight	
	S_1	S_2		S_1	S_2		S_1	S_2
R-L ASIS	25	10	R-L PSIS	15	10	R-L LTHI	1	1
R-L LEK	15	10	R-L MEK	15	10	R-L LSHA	1	1
R-L LM	15	10	R-L MM	15	10	R-L HEE	10	10
R-L MT5	1	1	R-L MT2	4	10			

*Note:* S\_1 and S\_2 refer to two different sets of marker weights. S\_1 was used to generate the results presented in this study. R-L are for Right-Left, ASIS is for anterior superior iliac spine, PSIS is for posterior superior iliac spine, LTHI is for lateral thigh, LEK is for lateral epicondyle of the knee, MEK is for medial epicondyle of the knee, LSHA is for lateral shank, LM is for lateral malleolus, MM is for medial malleolus, HEE is for heel, MT5 is for fifth meta tarsal, and MT2 is for second meta tarsal.

**Table S3:** Marker weights used during inverse kinematics in OpenSim and Human Body Model (S\_a only).

Marker	Weight		Marker	Weight		Marker	Weight	
	S_a	S_b		S_a	S_b		S_a	S_b
R-L ASIS	1	3	R-L PSIS	1	2.2	R-L LTHI	1	1
R-L LEK	1	2	R-L MEK	0	1	R-L LSHA	1	1
R-L LM	1	1	R-L MM	0	1	R-L HEE	1	1.2
R-L MT5	1	1	R-L MT2	1	1.2			

*Note:* S\_a and S\_b refer to two different sets of marker weights. S\_a was used to generate the results presented in this study. R-L are for Right-Left, ASIS is for anterior superior iliac spine, PSIS is for posterior superior iliac spine, LTHI is for lateral thigh, LEK is for lateral epicondyle of the knee, MEK is for medial epicondyle of the knee, LSHA is for lateral shank, LM is for lateral malleolus, MM is for medial malleolus, HEE is for heel, MT5 is for fifth meta tarsal, and MT2 is for second meta tarsal.

**Table S4:** Root mean square (RMS) marker error (cm) and maximum marker error (cm) during scaling in OpenSim.

Metric	Scaling setup	Subjects							mean ± std
		1	2	3	4	5	6	7	
RMS marker error (cm)	A	3.0	2.8	2.5	1.8	2.4	3.4	3.3	2.7 ± 0.5
		1.6*	1.7*	1.4*	1.0*	1.4*	1.7*	2.2*	1.6 ± 0.4*
	B	3.0	2.6	2.5	1.8	2.3	3.2	2.7	2.6 ± 0.4
		1.4*	1.3*	1.4*	1.0*	1.2*	1.2*	1.2*	1.2 ± 0.2*
	C	3.0	2.6	2.4	1.8	2.3	3.2	2.7	2.6 ± 0.4
		1.4*	1.3*	1.3*	0.9*	1.2*	1.2*	1.2*	1.2 ± 0.2*
Max. marker error (cm)	A	6.9	6.3	6.7	5.2	7.3	8.0	8.2	6.9 ± 1.0
		2.2*	3.1*	2.4*	2.1*	2.5*	2.9*	4.9*	2.9 ± 1.0*
	B	7.2	6.7	7.0	5.2	7.7	8.3	7.4	7.1 ± 1.0
		2.1*	2.6*	2.4*	2.1*	2.3*	1.9*	2.1*	2.2 ± 0.2*
	C	7.3	6.5	6.7	5.2	7.4	8.2	7.4	7.0 ± 0.9
		2.1*	2.7*	2.4*	2.0*	2.4*	1.9*	1.9*	2.2 ± 0.3*
Max. marker error (marker)	A	R LTHI	R LTHI	R LTHI	R LTHI	R LTHI	R LSHA	L LSHA	
		R LEK*	L PSIS*	R MT5*	R MT5*	L PSIS*	L PSIS*	L PSIS*	
	B	R LTHI	R LTHI	R LTHI	R LTHI	R LTHI	L LTHI	L LSHA	
		R LEK*	L MEK*	R MT5*	R MT5*	R MT5*	R LM*	L PSIS*	
	C	R LTHI	R LTHI	R LTHI	R LTHI	R LTHI	L LTHI	L LSHA	
		R LEK*	L MEK*	R MT5*	R MT5*	R MT5*	R LM*	L PSIS*	

*Note:* Scaling setup A scales the pelvis uniformly and uses the set of markers S\_1 (see table S2). Scaling setup B scales the pelvis non-uniformly and uses the set of markers S\_1 (see table S2). Scaling setup C scales the pelvis non-uniformly and uses the set of markers S\_2 (see table S2). For the maximum marker error, the corresponding marker is reported: R-L are for Right-Left, LTHI is for lateral thigh, LSHA is for lateral shank, LEK is for lateral epicondyle of the knee, PSIS is for posterior superior iliac spine, MT5 is for fifth meta tarsal, and LM is for lateral malleolus. \* indicates results excluding non-bony landmark markers (i.e. R-L LTHI and R-L LSHA). Scaling setup B was used to generate the results presented in this study.

**Table S5:** Absolute difference (degrees) in joint kinematics averaged over the gait cycle and the 14 representative trials between different setups.

Degree of freedom	Setups being compared			
	A vs B	A vs C	B vs C	B vs D
<b>Sagittal plane hip</b>	<b>2.0 ± 1.4</b>	<b>1.7 ± 1.2</b>	<b>1.8 ± 2.0</b>	<b>0.5 ± 0.3</b>
<b>Frontal plane hip</b>	<b>0.4 ± 0.3</b>	<b>0.5 ± 0.4</b>	<b>0.4 ± 0.4</b>	<b>0.7 ± 0.4</b>
<b>Transversal plane hip</b>	<b>0.6 ± 0.6</b>	<b>0.9 ± 0.6</b>	<b>0.5 ± 0.4</b>	<b>0.3 ± 0.2</b>
<b>Sagittal plane knee</b>	<b>0.8 ± 0.6</b>	<b>1.0 ± 0.5</b>	<b>0.4 ± 0.5</b>	<b>0.3 ± 0.2</b>
<b>Sagittal plane ankle</b>	<b>1.0 ± 1.0</b>	<b>2.1 ± 1.4</b>	<b>1.4 ± 1.2</b>	<b>0.4 ± 0.3</b>
<b>Subtalar</b>	<b>1.4 ± 1.3</b>	<b>1.8 ± 1.8</b>	<b>2.1 ± 1.8</b>	<b>0.4 ± 0.3</b>

*Note:* Setup A scales the pelvis uniformly, uses the set of markers S\_1 (see Table S2) for scaling, and uses the set of markers S\_a (see Table S3) for inverse kinematics. Setup B scales the pelvis non-uniformly, uses the set of markers S\_1 (see Table S2) for scaling, and uses the set markers S\_a (see Table S3) for inverse kinematics. Setup C scales the pelvis non-uniformly, uses the set of markers S\_2 (see Table S2) for scaling, and uses the set of markers S\_a (see Table S3) for inverse kinematics. Setup D scales the pelvis non-uniformly, uses the set of markers S\_1 (see Table S2) for scaling, and uses the set of markers S\_b (see Table S3) for inverse kinematics. Setup B was used to generate the results presented in this study. The largest effect of the scaling setup was 2.1 degrees for the ankle and subtalar joints (A vs C and B vs C, respectively). The largest effect of the inverse kinematic setup was 0.7 degrees for the frontal plane hip joint (B vs D).

